Biogeosciences Discuss., doi:10.5194/bg-2017-118, 2017
Manuscript under review for journal Biogeosciences
Discussion started: 13 April 2017

Biogeosciences Discussions Open Access EGU

Primary production sensitivity to phytoplankton light attenuation parameter increases with transient forcing

Karin F. Kvale[1] and Katrin J. Meissner[2,3]

[1]GEOMAR Helmholtz-Zentrum für Ozeanforschung Kiel, Düsternbrooker Weg 20, D-24105 Kiel, Germany
[2]Climate Change Research Centre, Level 4 Mathews Building, UNSW, Sydney, NSW, Australia
[3]ARC Centre of Excellence for Climate System Science

Correspondence to: K. Kvale (kkvale@geomar.de)

Abstract. Treatment of the underwater light field in ocean biogeochemical models has been attracting increasing interest, with some models moving towards more complex parameterisations. A simple test of the sensitivity of a typical, highly simplified parameterisation, to adjustment of the phytoplankton light attenuation parameter using both steady-state and future projections reveals a range of values to which the model primary production is relatively insensitive in steady-state but to which it becomes increasingly sensitive under climate forcing. Parameter value choice can determine the magnitude and sign of global net primary production trends in a high CO_2 forcing scenario. Ocean oxygen is particularly sensitive to parameter choice. With climate forcing, two simulations establish a strong biogeochemical feedback between the Southern Ocean and low latitude Pacific that highlights the potential for regional teleconnection and serves as a reminder that shifts in fundamental properties (e.g., light attenuation by phytoplankton) over deep time have the potential to alter biogeochemical climate.

1 Introduction

Treatment of marine light availability for photosynthesis in biogeochemical compartments of ocean general circulation models (OGCMs) has largely avoided careful scrutiny until recently (e.g., Dutkiewicz et al. 2015; Kim et al. 2015; Gregg and Rousseaux 2016). These models typically use simplified, empirically-based parameterisations of phytoplankton growth rates related to photosynthetically available radiation (PAR) based on the state of the science in the 1970s and 1980s. The OGCM in the University of Victoria Earth System Climate Model (UVic ESCM; Weaver et al. 2001; Eby et al. 2009) is one example. In it, the irradiance (I) at each depth level is calculated as (Schmittner et al., 2005; Kirk, 1983):

$$I = I_{z=0}\mathrm{PAR}\exp(-k_w\tilde{z} - k_c\int_0^{\tilde{z}}(P + Diaz)dz)\cdot[1 + a_i(\exp(-k_i(h_i + h_s)) - 1)] \quad (1)$$

where PAR stands for photosynthetically available radiation, k_w, k_c, and k_i are light attenuation coefficients for water, phytoplankton (diazotrophs and general phytoplankton), and ice, $\tilde{z}$ is the effective vertical coordinate, a_i is the fractional sea ice cover, and h_i and h_s are calculated sea ice and snow cover thicknesses. Phytoplankton concentration (P and $Diaz$) is expressed in a base unit of mmol N m^{-3}. Light attenuation coefficients k_w and k_i have the unit of m^{-1}, but light attenuation by phytoplankton is dependent on phytoplankton concentration (Kirk, 1975) and k_c is expressed in units of (m mmol N $m^{-3})^{-1}$.

Biogeosciences Discuss., doi:10.5194/bg-2017-118, 2017
Manuscript under review for journal Biogeosciences
Discussion started: 13 April 2017

However, k_c cannot be considered to represent the light attenuation of phytoplankton only, but also represents the attenuation of constituents that are assumed to covary with phytoplankton (i.e., particulate and dissolved inorganic and organic materials). Light attenuation coefficients are classified as apparent optical properties (AOP) because they represent the combined effect of the inherent optical properties (IOP) of the medium (e.g., seawater or phytoplankton cells) and the optical properties of the radiation field (see Kirk, 1983; Falkowski and Woodhead, 1992, and associated references). While it was recognized early on that a rigorous description of the spectral composition of the underwater light field must separate effects of IOP from the radiation field, early measurements emphasised AOP because of technological limitations as well as for a lack of data resolving the IOP of seawater constituents (Kirk, 1983). Research into the IOP of these constituents has since benefitted from continuously improving analytical tools including satellite remote sensing, whose algorithms depend on their resolution (Sathyendranath and Platt, 2007). Phytoplankton IOP are species-specific (e.g., Stramski et al., 2001). Of the major seawater constituents, non-algal particles contribute the most to light scattering and attenuation, and picoplankton are the primary phytoplankton light absorbers (Stramski et al., 2001; Fujii et al., 2007), though their contribution to absorption is possibly exceeded by coloured dissolved organic matter (CDOM) (Siegel et al., 2005; Fujii et al., 2007).

Recent work has highlighted what we potentially lose in our OGCMs, and hence our earth system models (ESMs) as well, by neglecting explicit radiative transfer and IOP. Decomposing the calculation of underwater irradiance into IOP, resolving a variable number of radiative wavebands, and then testing three parameterisations of light limitation of phytoplankton growth in a one dimensional ecosystem model comparable to observational data show a model resolving multiple wavebands and a spectral sensitivity in photosynthesis outperformed a simple parameterisation (Kettle and Merchant, 2008) similar to Equation 1. Choice in parameterisation of spectral resolution can contribute percentage errors of up to 200% (Kettle and Merchant, 2008). Not including a radiative transfer model in an OGCM can reduce global nitrate by 33% and chlorophyll by 24%, and bring about large changes in phytoplankton biogeography, even when there is no change in total irradiance (Gregg and Rousseaux, 2016). Dutkiewicz et al. (2015) offer the most complicated model analysis, and demonstrate explicitly resolving radiative transfer and the IOP of phytoplankton types, detritus, and CDOM in a three-dimensional ocean model can improve model performance against observational data. Their sensitivity analysis demonstrates complex feedbacks between light, phytoplankton attributes, and biogeochemistry (Dutkiewicz et al., 2015).

Explicit radiative transfer and fully resolved IOP add computational expense to already expensive ESMs. Since empirically-based AOP parameterisations are still widely used and economical, it is useful to test their limitations and sensitivities. Including light attenuation by phytoplankton in an OGCM amplifies the seasonal cycle of temperature, mixed layer depth and ice cover by about 10% over neglecting it altogether (Manizza et al., 2005). Gnanadesikan and Anderson (2009) find the inclusion of light attenuation by chlorophyll in an OGCM alters physical water mass characteristics including a decrease in subsurface temperatures by over 2°C in the low latitudes. Kim et al. (2015) explore the biogeochemical consequences of differentiating light attenuation by CDOM and non-algal particles from that of chlorophyll in an ESM and find these components increased surface phytoplankton biomass by reducing levels of light at depth, which reduced deeper production and made more nutrients available at the surface. Two model simulations with-and-without CDOM and non-algal particle light attenuation differ by 9% in the global average biomass and 7% in the global carbon export flux at 200 meters depth (Kim et al., 2015). These are

Biogeosciences Discuss., doi:10.5194/bg-2017-118, 2017
Manuscript under review for journal Biogeosciences
Discussion started: 13 April 2017

modest changes with respect to other production and export parameters (e.g., remineralisation depth, Kwon et al. 2009), though regional sensitivities are stronger (Kim et al., 2015).

All of the studies mentioned above make their comparisons using models at steady-state. Dutkiewicz et al. (2015) highlighted the potential for complex feedbacks arising due to model treatment of light and optical properties, therefore it stands to reason such feedbacks may compound under climate change. A recent bug fix in the implementation of Equation 1 in the UVic ESCM prompted a hasty steady-state model re-evaluation, which then led to our more thorough assessment including climate change. Future implementation of a more complex radiative transfer and phytoplankton IOP model may be justified based on the conclusions of the authors above (e.g., Dutkiewicz et al., 2015), however the UVic ESCM (and other models of similar structure) is widely used in its current form and it is therefore worthwhile to assess and report on its current sensitivities.

2 Methods

The University of Victoria Earth System Climate Model (UVic ESCM, Weaver et al. 2001, Eby et al. 2009) version 2.9 is a coarse-resolution ($1.8^\circ \times 3.6^\circ \times 19$ ocean depth layers) ocean-atmosphere-biosphere-cryosphere-geosphere model. The biogeochemical compartment (Schmittner et al., 2005, 2008; Keller et al., 2012) is a nutrients-phytoplankton-zooplankton-detritus (NPZD) model with two phytoplankton types (general phytoplankton and diazotrophs), one zooplankton type, and chemical tracers nitrate, phosphate, dissolved inorganic carbon, alkalinity, and oxygen. The biogeochemistry is comprehensively assessed in Keller et al. (2012), however, the model has since been updated with several bug fixes and minor adjustments. Only one of the bug fixes is relevant to our study. In previous published versions of the model, the depth was incorrectly calculated for the light availability equation in a way that resulted in too much light in the first ocean depth level. This calculation is corrected here.

Our study examines model biogeochemical sensitivity to a spread of k_c values at both steady-state in a pre-industrial climate (atmospheric CO_2 concentration of 283.8 ppm), and to a climate forcing away from that equilibrium using historical atmospheric CO_2 changes, agricultural, volcanic, sulphate aerosol and CFC emissions, and changes to land ice and solar forcing applied from year 1800 to 2005 following Machida et al. (1995); Battle et al. (1996); Etheridge et al. (1996, 1998); Flückiger et al. (1999, 2004); Ferretti et al. (2005); Meure et al. (2006). From year 2005 to 2300 the models were forced using increasing CO_2 concentrations and radiative forcing from all non-CO_2 greenhouse gases, fractions of the land surface devoted to agricultural uses, and the direct effect of sulphate aerosols as an alteration of the surface albedo following "business-as-usual" RCP scenario 8.5 (RCP8.5, Riahi et al., 2007; Meinshausen et al., 2011). Solar insolation at the top of the atmosphere, wind stress, and wind fields varied seasonally (Kalnay et al., 1996), and the wind fields were geostrophically adjusted to air temperature anomalies (Weaver et al., 2001). The sediment and weathering models (Meissner et al., 2012) were not used. Model equilibration was achieved by integrating over 10,000 years prior to application of climate forcing.

The simplistic nature of Equation 1 makes our study highly idealised. Parameter k_w represents light attenuation of water and is fairly well-constrained to about 0.04 m^{-1} (Lorenzen, 1972), which is its assigned value in the model. The light attenuation of ice parameter is not examined here. Light attenuation by phytoplankton also implicitly accounts for attenuation of light by

Biogeosciences Discuss., doi:10.5194/bg-2017-118, 2017
Manuscript under review for journal Biogeosciences
Discussion started: 13 April 2017

covarying factors, with the current default model value applied to both diazotrophs and the single general phytoplankton type (Eqn. 1). The Schmittner et al. (2008) k_c value of 0.03 (m mmol N m^{-3})$^{-1}$ is probably derived from Fasham et al. (1990), but was increased in Keller et al. (2012) to 0.047 (m mmol N m^{-3})$^{-1}$. Light attenuation parameters are measured based on chlorophyll (commonly Chlorophyll a) concentration but the model uses nitrogen units, necessitating the application of an assumed conversion factor also implicit to k_c. Early tests of k_c at steady-state (e.g., Fasham et al., 1990) demonstrated low model biomass sensitivity to parameter value choice, and this has been the prevailing wisdom of biogeochemical modellers for over 20 years. Replacing the UVic ESCM default value with a different one might result in a k_c of 0.014 m^2(mg Chl a)$^{-1}$ (generally applicable, Lorenzen, 1972), 0.041 m^2(mg Chl a)$^{-1}$ (Southern Ocean, Bracher and Tilzer, 2001), or a range anywhere from 0.006–0.015 m^2(mg Chl a)$^{-1}$ assuming all phytoplankton represent mixes of specific species of dinoflagellates, calcifiers, or diatoms (Falkowski et al., 1985). However, even the simple assumption that k_c varies with chlorophyll concentration can be considered highly simplistic (Siegel et al., 2005). In practice, any value assigned to k_c is going to be highly model-dependent (e.g., 0.058 m^2(mg Chl a)$^{-1}$ in Wang et al., 2008). Conversion of these k_c values to nitrogen units using a recent overview of the data (Dutkiewicz et al., 2015) yields a range of 0.008–0.054 (m mmol N m^{-3})$^{-1}$ (though higher values in models existEvans and Parslow 1985 used a value of 0.12 (m mmol N m^{-3})$^{-1}$). For our test, we employ eight separate simulations using $k_c = 0.01$, 0.02, 0.03, 0.04, 0.05, 0.06, 0.07, and 0.08 (m mmol N m^{-3})$^{-1}$. In the following analysis, they will be referred to as 'K1-8', respectively.

3 Results

3.1 Pre-industrial equilibrium

Equilibrium primary production in the UVic ESCM shows modest sensitivity to the range of k_c values chosen. Figure 1 provides zonally averaged surface chlorophyll, calculated from model nitrogen units using a conversion factor of 1.59 following Schmittner et al. (2005). SeaWiFS satellite chlorophyll data from 1997-2007 (NASA Goddard Space Flight Center, Ocean Biology Processing Group), regridded to the model grid, are also included. All simulations overestimate chlorophyll with respect to observations in the tropics and the southern hemisphere middle latitudes, and underestimate chlorophyll at high latitudes. Model-observation RMSE reveals best agreement between SeaWiFS and K1 chlorophyll (RMSE 0.837) and worsening agreement with increasing k_c (Fig. 1). The simulation spread is slightest between 20 and 40°, where phytoplankton biomass is low. The Southern Ocean and tropics are the two regions where chlorophyll concentrations are most sensitive to k_c value (Figs. 1 and 2). In the Southern Ocean, K1 produces zonally averaged biomass concentrations more than 5 times larger than K8 because phytoplankton in K1 do not self-shade as strongly during the Austral summer, thereby allowing for a stronger seasonal cycle. In the stratified tropics, the effect is opposite in that K8 yields zonally averaged biomass concentrations of up to double K1 because stronger self-shading inhibits deeper photosynthesis (Fig. 1), making more nutrients available at the surface (Fig. 3, and as described previously by Kim et al. 2015).

Increasing k_c values reduces average surface alkalinity (Fig. 3) by about 50 μmol kg^{-1} globally, a response to low latitude increasing surface primary production rates (including a stronger carbonate pump) with higher k_c values. Deep ocean alkalinity

Biogeosciences Discuss., doi:10.5194/bg-2017-118, 2017
Manuscript under review for journal Biogeosciences
Discussion started: 13 April 2017

is less sensitive to k_c value, though the average deep Pacific also shows a range of about 50 μmol kg^{-1} and the Southern Ocean varies by about 25 μmol kg^{-1}. Deep ocean DIC, however, is more sensitive to choice of k_c value (Fig. 3). K4-K8 DIC ranges in basin averages less than 30 μmol kg^{-1} but sensitivity increases at lower k_c values. K1 deep DIC values are about 40 μmol kg^{-1} higher in the global average, Pacific, and Southern Ocean basins than K2. These higher deep DIC values are a consequence of higher surface primary production in the high latitudes owing to a weaker self-shading effect, which increase carbon and nutrient export to the deep ocean. Phosphate and nitrate basin-averaged profiles show a range of values generally proportionate to the range in DIC, with drivers of the differences being the same (lower k_c values yield higher surface production, lower surface nutrients, and higher deep ocean nutrients, Fig. 3). Likewise, deep ocean oxygen is lower for lower k_c values (more deep ocean remineralisation), Fig. 3. The global average deep ocean oxygen concentration has a range of about 100 mmol m^{-3}, which is about half of the average deep ocean content. The Southern Ocean and Pacific show similar oxygen sensitivity.

Which k_c value performs the "best" with respect to biogeochemical observations is not quantified here, but generally K4 and above perform better in the deep ocean than K1-K3. Observations included in Figure 3 are from the World Ocean Atlas climatology (Garcia et al., 2010a, b) and GLODAP (Key et al., 2004).

3.2 RCP 8.5 transient simulation

Figure 4 plots the increase in atmospheric CO_2 concentration from 283.8 ppm to 1962 ppm over the course of the transient integration. The physical response is the same across all simulation configurations and closely follows that described in Kvale et al. (2015). Zonally averaged ocean surface temperatures rise by as much as 10°C, global maximum meridional overturning reduces from 20 to 9 Sverdrups (not shown), and widespread near-surface stratification occurs (Fig. 4). The phytoplankton and zooplankton respond to surface warming by increasing metabolic rates, and microbial fast recycling in the near-surface increases (Kvale et al., 2015). Stratification reduces the availability of nutrients in the near-surface. The global response in net primary production (NPP) until about the year 2100 depends on the simulation, with K1-K6 showing a decline, and K7 and K8 showing no change and an increase in NPP, respectively. After about year 2100, global NPP in K4-K8 increases linearly, while global NPP increases at a declining rate in K1-K3.

Before about the year 2100, physical limitation of nutrients is the dominant driver of changes in global NPP (Kvale et al., 2015). Declining global NPP in the simulations with relatively weaker self-shading (K1-K6) is a result of increasingly oligotrophic conditions in the low latitudes and the northern hemisphere, where these simulations had relatively lower pre-industrial near-surface nutrient concentrations owing to deeper primary production. Relatively lower starting concentrations causes the biology in these simulations to be relatively more sensitive to an increase in stratification. Figure 5 repeats Figure 1 for years 2100 and 2300 and shows a decline in biomass in both of these regions for these simulations. These declines are not offset by increasing biomass in the Southern Ocean, which is driven by regional increasing temperature, wind-driven overturning, and nutrient remineralisation (Kvale et al., 2015). The pre-2100 increase in global NPP in K8 is due primarily to increasing biomass north of 60°N and modest increases in biomass in the low latitudes (Fig. 5). Biomass in K7 and K8 is relatively less sensitive to increasing stratification because their high k_c values limit primary production to the very near-surface, thereby

Biogeosciences Discuss., doi:10.5194/bg-2017-118, 2017
Manuscript under review for journal Biogeosciences
Discussion started: 13 April 2017

raising surface nutrient concentrations and allowing the phytoplankton to be less reliant on resupply of nutrients from deeper waters.

After about year 2100, physical limitation of nutrients becomes a less important driver of changes in global NPP than temperature-enhanced biological processes (Kvale et al., 2015). Increasing global NPP in all simulations is dominated by increasing biomass in the Southern Ocean, though biomass also increases modestly in the low latitudes for K3-K8 (Fig. 5). The drivers of change in NPP in the Southern Ocean are the same as those mentioned earlier, with alleviation of light and temperature limitations increasing production rates. Declines in northern hemisphere NPP do not offset the Southern Ocean increases, however the three simulations with the weakest self-shading (K1-K3) also show declining rates of global NPP increase due in part to declines in the northern hemisphere NPP.

Model spread in biomass and NPP response generally increases with radiative forcing. Change in global NPP differs by about 2.5 Pg C y^{-1} by 2100 (more than 100% of the total change in NPP at 2100 for all simulations) and k_c parameter choice can determine the sign of the change. This is true even if only considering the k_c parameters offering the better fits to pre-industrial nutrient and carbon observations (K4-K8). By 2300 this spread has increased to about 7 Pg C y^{-1} across all simulations, and 4 Pg C y^{-1} between K4 and K8. Differences in simulated response in Southern Ocean chlorophyll are the most remarkable, with K1 having an average chlorophyll concentration at 60°S of over 2 mg m^{-3} higher than K8 at 2100 (a concentration more than four times higher than K8) that has increased to a difference of almost 2.5 mg m^{-3} higher by 2300.

The biogeochemical consequences of k_c parameter choice at years 2100 and 2300 are shown for major ocean basins in Figures 6 and 7. Unsurprisingly for the time period considered, most basins and biogeochemical quantities retain the pre-industrial spread in average basin profiles when increasing CO_2 forcing. The prime exceptions are the abyssal Southern Ocean, which displays modestly increasing simulation spread with time in all biogeochemical quantities below about 4000 meters, and oxygen throughout the Southern Ocean. Models K1-K3 are principally responsible for the simulation divergence in these regions, while higher k_c parameter choices respond more uniformly. Map views of surface and near-surface simulated spread (K1-K8) better reflect trends at hundred-year timescales (Fig. 7). For all biogeochemical quantities, simulated spread at the surface increases with time. K1 has generally lower pre-industrial NPP than K8 that also increases less over the transient simulation, therefore surface alkalinity and DIC rise faster in K1, with large parts of the low latitudes showing a difference exceeding 70 μmol kg^{-1} alkalinity and 60 μmol kg^{-1} DIC by 2300. Surface phosphate and nitrate concentrations remain generally higher in K8 than in K1 throughout the transient simulation as a result of the shallower and greater NPP. Model surface spread in the Southern Ocean increases by about 0.2 mmol P m^{-3} and 2 mmol N m^{-3} between 2100 and 2300. The difference between K1 and K8 Southern Ocean oxygen at 300 meters is up to 100 mmol m^{-3} by 2100, but by 2300 that difference has grown to a maximum of 160 mmol m^{-3}. All simulations experience a loss in oxygen due to warming and increasing remineralisation, but K1 and K2 additionally experience denitrification in the Southern Ocean (not shown) as a result of very high primary production in the region and already lower oxygen concentrations at steady-state. This denitrification establishes a nutrient feedback with the low latitude Pacific that reduces Southern Ocean oxygen further (Fig. 8), thus producing a strong regional decline in oxygen despite K1 and K2 showing weaker global NPP trends than the other simulations. The feedback starts with increased stratification in the low-latitude Pacific, which limits nitrate availability for local primary production. As a result, more phos-

Biogeosciences Discuss., doi:10.5194/bg-2017-118, 2017
Manuscript under review for journal Biogeosciences
Discussion started: 13 April 2017

phate begins to advect into the Southern Ocean, where it fertilizes phytoplankton growth. Warming seawater increases both primary production and remineralisation rates. Phytoplankton in K1 and K2 are only weakly inhibited by self-shading, and the resulting large increases in primary production leads to the consumption of enough oxygen that denitrification establishes in the Southern Ocean. Denitrification reduces the flow of nitrate in intermediate water back into the low latitude Pacific, which becomes even more nitrate-limited.

4 Discussion

Our results show choice of k_c value for our model matters little for primary production in equilibrium tests within a range above 0.04 (m mmol N m^{-3})$^{-1}$. Primary production sensitivity increases with lower k_c values, with reduced shading sensitivity allowing for a stronger seasonal cycle in the high latitudes, producing higher carbon and nutrient export. Equilibrium deep ocean oxygen is particularly sensitive to the application of k_c values between 0.01 and 0.03 (m mmol N m^{-3})$^{-1}$.

Model spread increases in our transient simulations, and k_c parameter choice can determine the sign as well as the magnitude of the global NPP response. Substantial differences in model behaviour occur even within the k_c range shown insensitive in equilibrium tests, and within the range performing best with respect to pre-industrial biogeochemical observations. That this is true is a general reminder of the potential omission of important tuning information when focusing only on steady-state models. These differences in model behaviour have biogeochemical consequences below the surface, with oxygen again showing particular sensitivity to parameter choice. A nutrient exchange feedback establishes in the two lowest k_c value simulations, substantially reducing Southern Ocean oxygen concentrations. While these two simulations performed less favourably with respect to gridded nutrient observations in a pre-industrial comparison and might therefore be considered less reliable representations of the modern ocean, they performed best against SeaWiFS chlorophyll data, which might point to needed additional export or remineralisation parameter adjustments to tune the deep ocean. It is worth noting this feedback occurs because: 1) it highlights the potential for strong biogeochemical teleconnection between the Southern Ocean and the low latitude Pacific, and 2) both light attenuation characteristics of dominant phytoplankton and ocean oxygen volatility have changed over geologic timescales (e.g., Katz et al., 2004; Lenton et al., 2014). A recent model study by Meyer et al. (2016) explored the sensitivity of oxygen to e-folding depth of remineralisation and total phosphate inventory and hypothesized an increase in remineralisation depth has occurred over the Phanerozoic alongside a stabilisation of ocean oxygen inventory. Our tests demonstrate another potential mechanism (evolutionary increase in light attenuation characteristics by dominant phytoplankton) for the increase in ocean oxygen inventory in steady-state conditions as well as stabilisation of oxygen under rapid climate change.

5 Conclusions

The typical, highly simplistic parameterisations of underwater light availability used in climate and ocean models to calculate primary production and associated chemistry (alkalinity, DIC, nitrate, phosphate, and oxygen) contain substantial sensitivity to light attenuation parameter. This applies both in steady-state and when using forced biogeochemistry for the range of val-

ues tested here. This sensitivity can grow with climate forcing as complex biogeochemical feedbacks develop, with primary production and ocean oxygen being especially susceptible to parameter choice. Our study highlights the need to assess biogeochemical models under transient as well as equilibrium conditions. In addition, the biogeochemical feedback we describe in two of our transient tests also serves as a reminder that even seemingly small events, like the emergence of shell-secreting phytoplankton, could have potentially large biogeochemical consequences just by altering the light field.

6 Code availability

Model data and figure scripts are available from https://thredds.geomar.de/thredds/catalog/open_access/kvale_meissner_2017_bg/catalog.html. Model code is available from the authors upon request.

Author contributions. K. Kvale designed and implemented the experiment, and wrote the paper with comments by K. Meissner. K. Kvale and K. Meissner interpreted the model results.

Acknowledgements. Computing resources were provided by Kiel University. SeaWiFS data were provided by the Ocean Biology Processing Group at NASA.

References

Battle, M., Bender, M., Sowers, T., Tans, P., Butler, J., Elkins, J., Ellis, J., Conway, T., Zhang, N., Lang, P., and Clarke, A.: Atmospheric gas concentrations over the past century measured in air from firn at the South Pole, Nature, 383, 231–235, doi:10.1038/383231a0, 1996.

Bracher, A. and Tilzer, M.: Underwater light field and phytoplankton absorbance in different surface water masses of the Atlantic sector of the Southern Ocean, Polar Biology, 24, 687–696, doi:10.1007/s003000100269, 2001.

Dutkiewicz, S., Hickman, A. E., Jahn, O., Gregg, W. W., Mouw, C. B., and Follows, M. J.: Capturing optically important constituents and properties in a marine biogeochemical and ecosystem model, Biogeosciences, 12, 4447–4481, doi:10.5194/bg-12-4447-2015, 2015.

Eby, M., Zickfeld, K., Montenegro, A., Archer, D., Meissner, K. J., and Weaver, A. J.: Lifetime of anthropogenic climate change: Millennial time scales of potential CO2 and surface temperature perturbations, Journal of Climate, 22, 2501–2511, doi:10.1175/2008JCLI2554.1, 2009.

Etheridge, D., Steele, L., Langenfelds, R., Francey, R., Barnola, J., and Morgan, V.: Natural and anthropogenic changes in atmospheric CO2 over the last 1000 years from air in Antarctic ice and firn, Journal of Geophysical Research-Atmospheres, 101, 4115–4128, doi:10.1029/95JD03410, 1996.

Etheridge, D., Steele, L., Francey, R., and Langenfelds, R.: Atmospheric methane between 1000 AD and present: Evidence of anthropogenic emissions and climatic variability, Journal of Geophysical Research-Atmospheres, 103, 15 979–15 993, doi:10.1029/98JD00923, 1998.

Evans, G. T. and Parslow, J. S.: A model of annual plankton cycles, Biological Oceanography, 3, 327–347, doi:10.1016/0198-0254(85)92902-4, 1985.

Falkowski, P. and Woodhead, A., eds.: Primary productivity and biogeochemical cycles in the sea, Proceedings of the conference on primary productivity and biogeochemical cycles in the sea, Brookhaven National Laboratory, Plenum Press, 1992.

Falkowski, P. G., Gan, R., and Wyman, K.: Growth-irradiance relationships in phytoplankton, Limnology and Oceanography, 30, 311–321, 1985.

Fasham, M. J. R., Ducklow, H. W., and McKelvie, S. M.: A nitrogen-based model of plankton dynamics in the oceanic mixed layer, Journal of Marine Research, 48, 591–639, doi:10.1357/002224090784984678, 1990.

Ferretti, D., Miller, J., White, J., Etheridge, D., Lassey, K., Lowe, D., Meure, C., Dreier, M., Trudinger, C., van Ommen, T., and Langenfelds, R.: Unexpected changes to the global methane budget over the past 2000 years, Science, 309, 1714–1717, doi:10.1126/science.1115193, 2005.

Flückiger, J., Dällenbach, A., Blunier, T., Stauffer, B., Stocker, T. F., Raynaud, D., and Barnola, J.-M.: Variations in atmospheric N2O concentration during abrupt climatic changes, Science, 285, 227–230, doi:10.1126/science.285.5425.227, 1999.

Flückiger, J., Blunier, T., Stauffer, B., Chappellaz, J., Spahni, R., Kawamura, K., Schwander, J., Stocker, T. F., and Dahl-Jensen, D.: N2O and CH4 variations during the last glacial epoch: Insight into global processes, Global Biogeochemical Cycles, 18, doi:10.1029/2003GB002122, 2004.

Fujii, M., Boss, E., and Chai, F.: The value of adding optics to ecosystem models: a case study, Biogeosciences, 4, 817–835, doi:10.5194/bg-4-817-2007, http://www.biogeosciences.net/4/817/2007/, 2007.

Garcia, H., Locarnini, R. A., Boyer, T. P., Antonov, J., Baranova, O., Zweng, M. M., and Johnson, D.: World Ocean Atlas 2009, Volume 3: Dissolved Oxygen, Apparent Oxygen Utilization, and Oxygen Saturation, Tech. rep., NOAA Atlas NESDIS 70, U.S. Government Printing Office, Washington, D.C., 2010a.

Garcia, H., Locarnini, R. A., Boyer, T. P., Antonov, J., Zweng, M. M., Baranova, O., and Johnson, D.: World Ocean Atlas 2009, Volume 4: Nutrients (phosphate, nitrate, silicate), Tech. rep., NOAA Atlas NESDIS 71, U.S. Government Printing Office, Washington, D.C., 2010b.

Gnanadesikan, A. and Anderson, W. G.: Ocean water clarity and the ocean general circulation in a coupled climate model, Journal of Physical Oceanography, 39, 314–332, doi:10.1175/2008JPO3935.1, 2009.

Gregg, W. W. and Rousseaux, C. S.: Directional and spectral irradiance in ocean models: Effects on simulated global phytoplankton, nutrients, and primary production directional and spectral irradiance in ocean models, Front. Mar. Sci, 3, 2403 389–240, doi:10.3389/fmars.2016.00240, 2016.

Kalnay, E., Kanamitsu, M., Kistler, R., Collins, W., Deaven, D., Gandin, L., Iredell, M., Saha, S., White, G., Woollen, J., Zhu, Y., Chelliah, M., Ebisuzaki, W., Higgins, W., Janowiak, J., Mo, K., Ropelewski, C., Wang, J., Leetmaa, A., Reynolds, R., Jenne, R., and Joseph, D.: The NCEP/NCAR 40-year reanalysis project, Bulletin of the American Meteorological Society, 77, 437–471, doi:10.1175/1520-0477(1996)077<0437:TNYRP>2.0.CO;2, 1996.

Katz, M. E., Finkel, Z. V., Grzebyk, D., Knoll, A. H., Paul, G., and Falkowski, P. G.: Evolutionary trajectories and biogeochemical impacts of marine eukaryotic phytoplankton, Annual Review of Ecology, Evolution and Systematics, 35, 523–556, doi:10.2307/annurev.ecolsys.35.112202.30000020, 2004.

Keller, D. P., Oschlies, A., and Eby, M.: A new marine ecosystem model for the University of Victoria Earth System Climate Model, Geoscientific Model Development, 5, 1195–1220, doi:10.5194/gmd-5-1195-2012, 2012.

Kettle, H. and Merchant, C. J.: Modeling ocean primary production: Sensitivity to spectral resolution of attenuation and absorption of light, Progress in Oceanography, 78, 135–146, doi:10.1016/j.pocean.2008.04.002, 2008.

Key, R., Kozyr, A., Sabine, C., Lee, K., Wanninkhof, R., Bullister, J., Feely, R., Millero, F., and Mordy, C.: A global ocean carbon climatology: Results from GLODAP, Global Biogeochemical Cycles, 18, 2004.

Kim, G. E., Pradal, M.-A., and Gnanadesikan, A.: Quantifying the biological impact of surface ocean light attenuation by colored detrital matter in an ESM using a new optical parameterization, Biogeosciences, 12, 5119–5132, doi:10.5194/bg-12-5119-2015, 2015.

Kirk, J. T. O.: A theoretical analysis of the contribution of algal cells to the attenuation of light within natural waters I: General treatment of suspensions of pigmented cells, New Phytologist, 75, 11–20, doi:10.1111/j.1469-8137.1975.tb01366.x, 1975.

Kirk, J. T. O.: Light and Photosynthesis in Aquatic Ecosystems, Cambridge University Press, 1983.

Kvale, K. F., Meissner, K. J., and Keller, D. P.: Potential increasing dominance of heterotrophy in the global ocean, Environmental Research Letters, 10, doi:10.1088/1748-9326/10/7/074009, 2015.

Kwon, E. Y., Primeau, F., and Sarmiento, J. L.: The impact of remineralization depth on the air–sea carbon balance, Nature Geoscience, 2, 630–635, doi:10.1038/ngeo612, 2009.

Lenton, T. M., Boyle, R. A., Poulton, S. W., Shields-Zhou, G. A., and Butterfield, N. J.: Co-evolution of eukaryotes and ocean oxygenation in the Neoproterozoic era, Nature Geosci, 7, 257–265, 2014.

Lorenzen, C.: Extinction of light in ocean by phytoplankton, Journal du Conseil, 34, 262–267, 1972.

Machida, T., Nakazawa, T., Fujii, Y., Aoki, S., and Watanabe, O.: Increase in the atmospheric nitrous-oxide concentration during the last 250 years, Geophysical Research Letters, 22, 2921–2924, doi:10.1029/95GL02822, 1995.

Manizza, M., Le Quere, C., Watson, A., and Buitenhuis, E.: Bio-optical feedbacks among phytoplankton, upper ocean physics and sea-ice in a global model, Geophysical Research Letters, 32, doi:10.1029/2004GL020778, 2005.

Meinshausen, M., Smith, S. J., Calvin, K., Daniel, J. S., Kainuma, M. L. T., Lamarque, J.-F., Matsumoto, K., Montzka, S. A., Raper, S. C. B., Riahi, K., Thomson, A., Velders, G. J. M., and van Vuuren, D. P. P.: The RCP greenhouse gas concentrations and their extensions from 1765 to 2300, Climatic Change, 109, 213–241, doi:10.1007/s10584-011-0156-z, 2011.

Meissner, K. J., McNeil, B. I., Eby, M., and Wiebe, E. C.: The importance of the terrestrial weathering feedback for multimillennial coral reef habitat recovery, Global Biogeochemical Cycles, 26, 2012.

Meure, M. C., Etheridge, D., Trudinger, C., Steele, P., Langenfelds, R., van Ommen, T., Smith, A., and Elkins, J.: Law Dome CO2, CH4 and N2O ice core records extended to 2000 years BP, Geophysical Research Letters, 33, doi:10.1029/2006GL026152, 2006.

Meyer, K. M., Ridgwell, A., and Payne, J. L.: The influence of the biological pump on ocean chemistry: Implications for long-term trends in marine redox chemistry, the global carbon cycle, and marine animal ecosystems, Geobiology, 14, 207–219, doi:10.1111/gbi.12176, 2016.

NASA Goddard Space Flight Center, Ocean Biology Processing Group: Sea-viewing Wide Field-of-view Sensor (SeaWiFS) Ocean Color Data, Annual 9km Chlorophyll, 1997-2010, https://oceandata.sci.gsfc.nasa.gov/SeaWiFS/Mapped/Annual/9km/chlor_a, 2015.

Riahi, K., Gruebler, A., and Nakicenovic, N.: Scenarios of long-term socio-economic and environmental development under climate stabilization, Technological Forecasting and Social Change, 74, 887–935, doi:10.1016/j.techfore.2006.05.026, 2007.

Sathyendranath, S. and Platt, T.: Spectral effects in bio-optical control on the ocean system, Oceanologia, 49, 5–39, 2007.

Schmittner, A., Oschlies, A., Giraud, X., Eby, M., and Simmons, H.: A global model of the marine ecosystem for long-term simulations: Sensitivity to ocean mixing, buoyancy forcing, particle sinking, and dissolved organic matter cycling, Global Biogeochemical Cycles, 19, 2005.

Schmittner, A., Oschlies, A., Matthews, H. D., and Galbraith, E. D.: Future changes in climate, ocean circulation, ecosystems, and biogeochemical cycling simulated for a business-as-usual CO2 emission scenario until year 4000 AD, Global Biogeochemical Cycles, 22, doi:10.1029/2007GB002953, 2008.

Siegel, D., Maritorena, S., Nelson, N., and Behrenfeld, M.: Independence and interdependencies among global ocean color properties: Reassessing the bio-optical assumption, Journal of Geophysical Research-Oceans, 110, doi:10.1029/2004JC002527, 2005.

Stramski, D., Bricaud, A., and Morel, A.: Modeling the inherent optical properties of the ocean based on the detailed composition of the planktonic community, Appl. Opt., 40, 2929–2945, doi:10.1364/AO.40.002929, 2001.

Wang, X. J., Le Borgne, R., Murtugudde, R., Busalacchi, A. J., and Behrenfeld, M.: Spatial and temporal variations in dissolved and particulate organic nitrogen in the equatorial Pacific: biological and physical influences, Biogeosciences, 5, 1705–1721, doi:10.5194/bg-5-1705-2008, 2008.

Weaver, A., Eby, M., Wiebe, E., Bitz, C., Duffy, P., Ewen, T., Fanning, A., Holland, M., MacFadyen, A., Matthews, H., Meissner, K., Saenko, O., Schmittner, A., Wang, H., and Yoshimori, M.: The UVic Earth System Climate Model: Model description, climatology, and applications to past, present and future climates, Atmosphere-Ocean, 39, 361–428, doi:10.1080/07055900.2001.9649686, 2001.

Biogeosciences Discuss., doi:10.5194/bg-2017-118, 2017
Manuscript under review for journal Biogeosciences
Discussion started: 13 April 2017

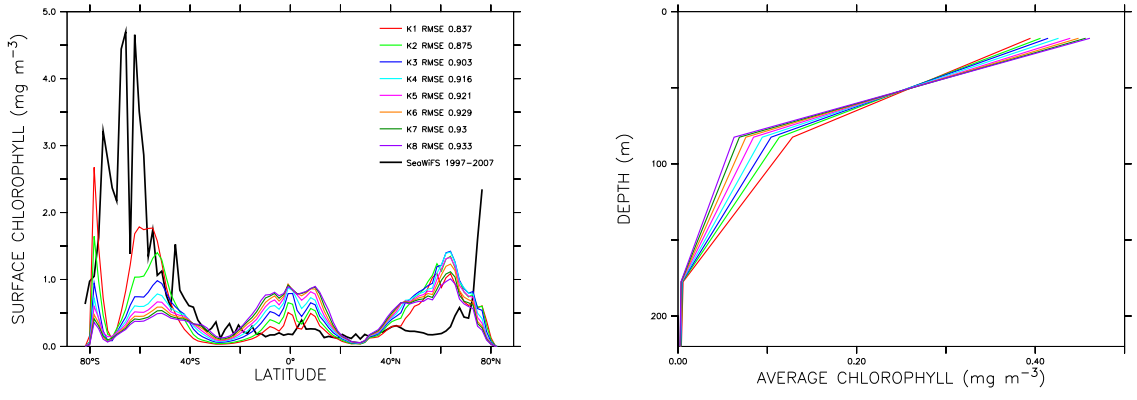

Figure 1. Anually averaged pre-industrial surface chlorophyll concentration (left), and chlorophyll concentration with depth (right).

Biogeosciences Discuss., doi:10.5194/bg-2017-118, 2017
Manuscript under review for journal Biogeosciences
Discussion started: 13 April 2017

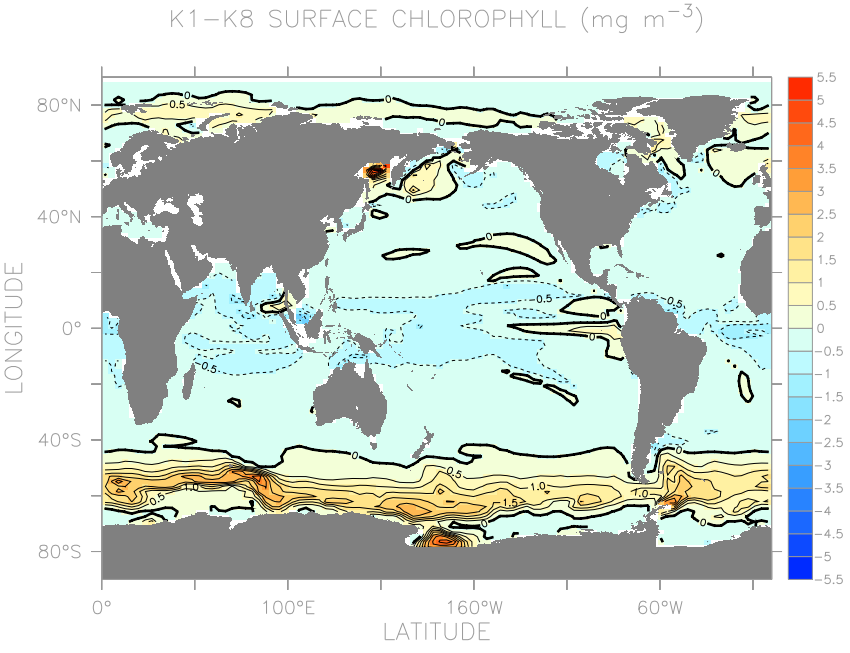

Figure 2. Anually averaged pre-industrial surface chlorophyll concentration difference between K1 and K8.

Biogeosciences Discuss., doi:10.5194/bg-2017-118, 2017
Manuscript under review for journal Biogeosciences
Discussion started: 13 April 2017

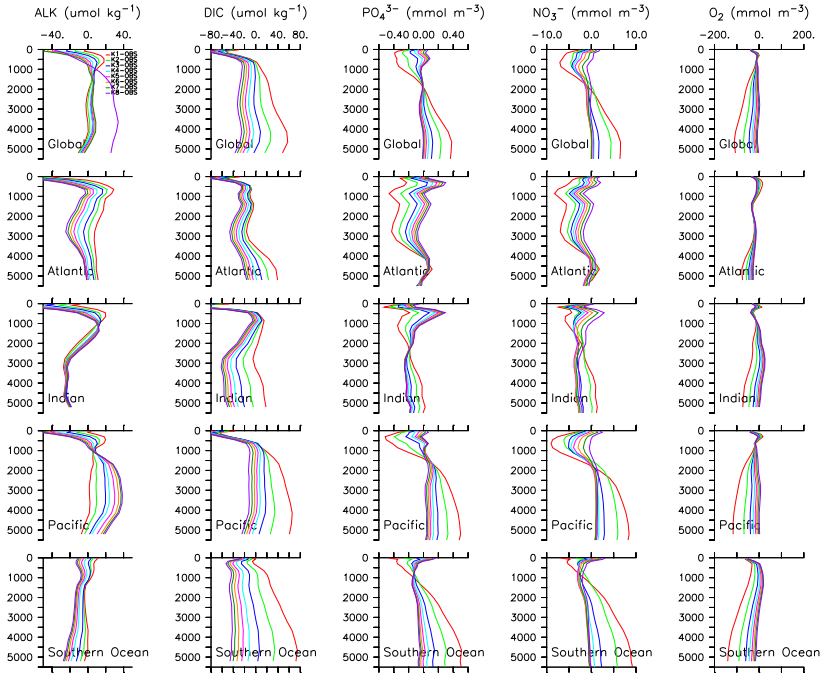

Figure 3. Steady-state biogeochemical tracer profiles averaged by ocean basin for all simulations and observations.

Biogeosciences Discuss., doi:10.5194/bg-2017-118, 2017
Manuscript under review for journal Biogeosciences
Discussion started: 13 April 2017

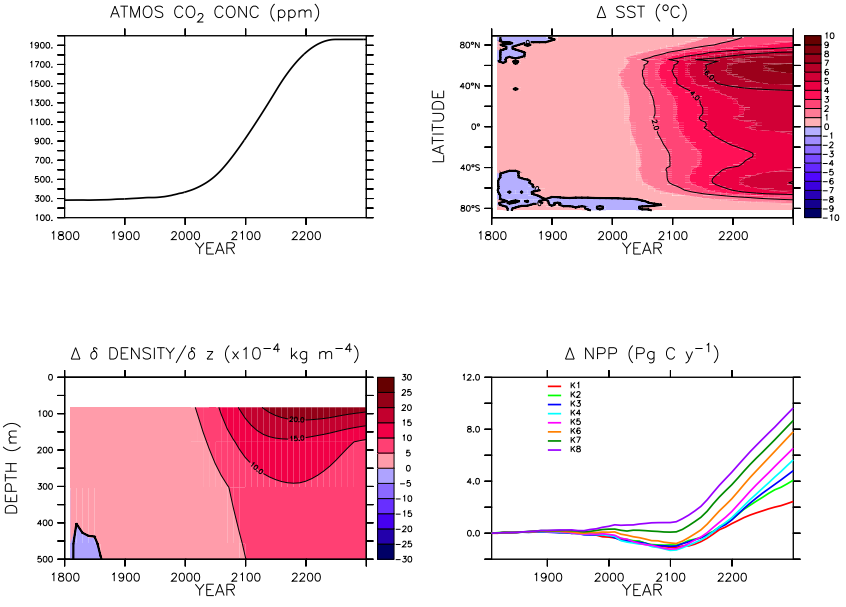

Figure 4. Atmospheric CO_2 concentration forcing of all simulations (top left). Zonally averaged change in sea surface temperature in all simulations (top right). Change in global average density gradient with depth in all simulations (bottom left). Change in globally integrated net primary production in all simulations (bottom right).

Biogeosciences Discuss., doi:10.5194/bg-2017-118, 2017
Manuscript under review for journal Biogeosciences
Discussion started: 13 April 2017

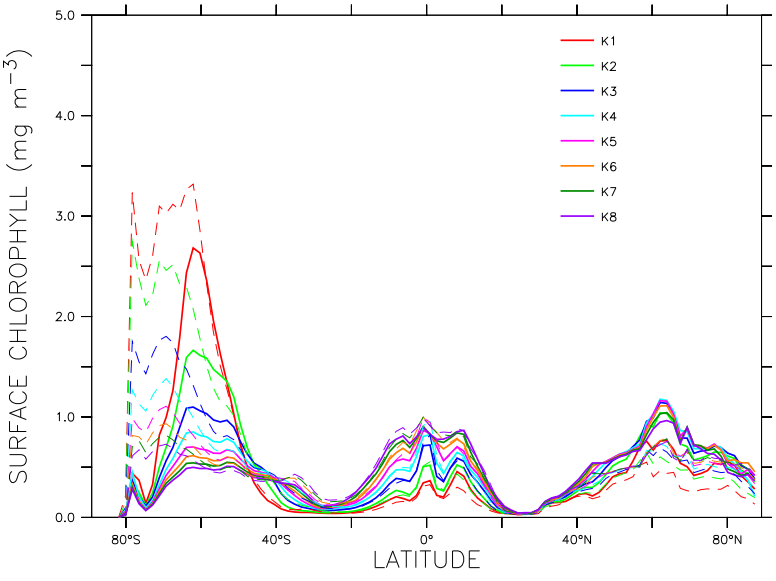

Figure 5. Anually averaged surface chlorophyll concentration at years 2100 (solid lines) and 2300 (dashed lines).

Biogeosciences Discuss., doi:10.5194/bg-2017-118, 2017
Manuscript under review for journal Biogeosciences
Discussion started: 13 April 2017

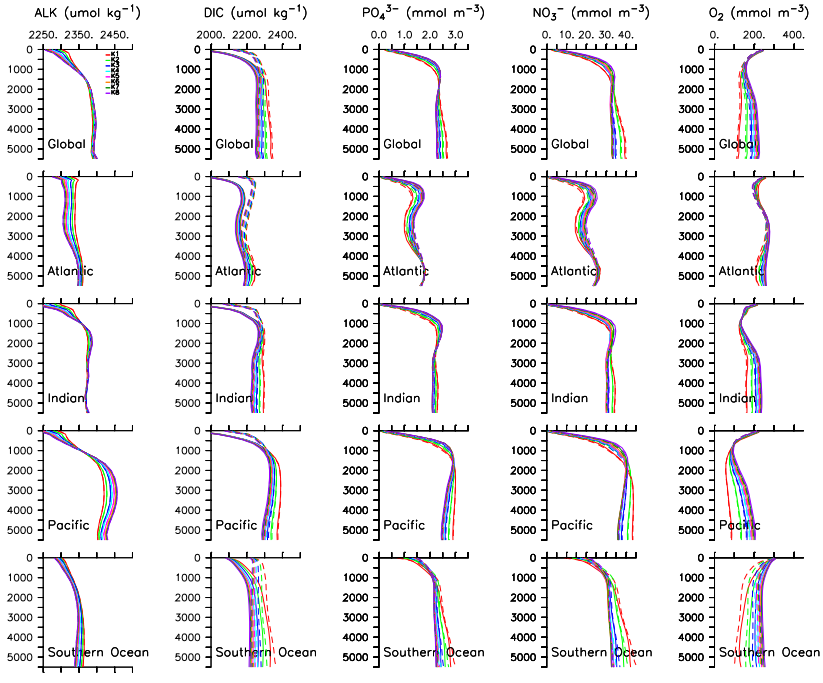

Figure 6. Biogeochemical tracer profiles averaged by ocean basin for all simulations at years 2100 (solid lines) and 2300 (dashed lines).

Biogeosciences Discuss., doi:10.5194/bg-2017-118, 2017
Manuscript under review for journal Biogeosciences
Discussion started: 13 April 2017

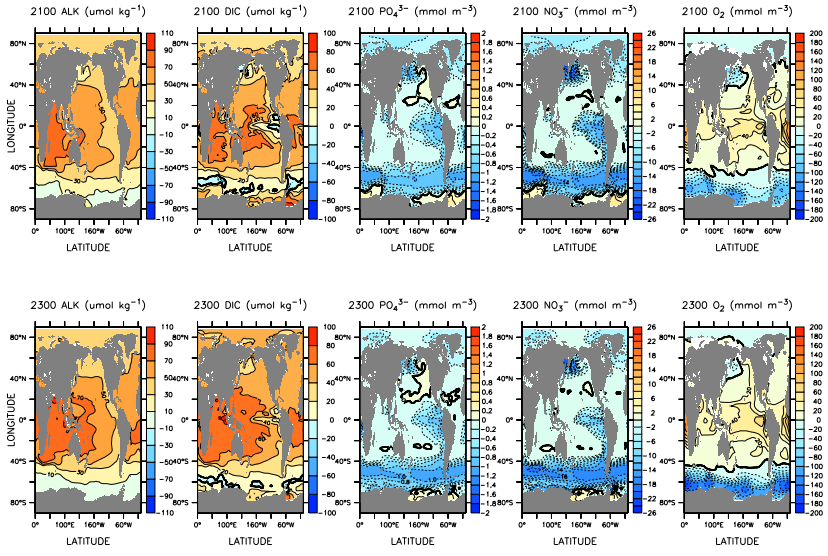

Figure 7. Anually averaged years 2100 and 2300 surface chemical concentration differences between K1 and K8. Oxygen differences are calculated at 300 meters depth.

Biogeosciences Discuss., doi:10.5194/bg-2017-118, 2017
Manuscript under review for journal Biogeosciences
Discussion started: 13 April 2017

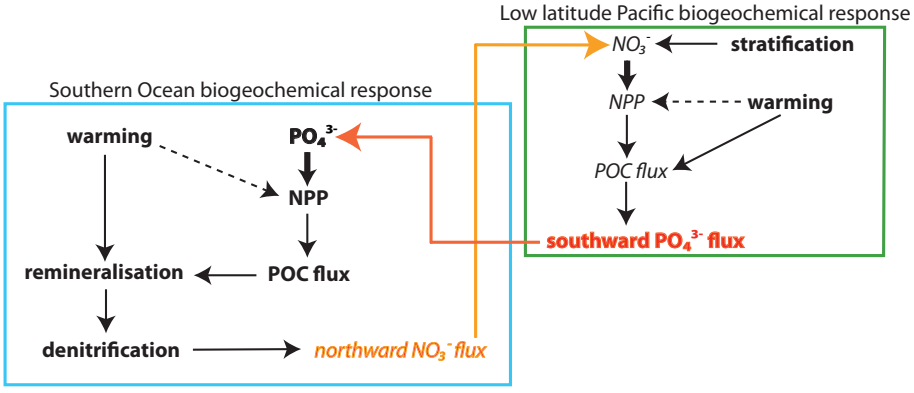

Figure 8. K1 and K2 feedback schematic in Southern Ocean and low latitude Pacific nutrients. Increases with climate change are represented in bold font. Decreases with climate change are represented in italic font. Regular font indicates little or no change with climate forcing. Bold arrows indicate the dominant factor influencing change in NPP. Dashed arrows indicate the secondary factor influencing change in NPP. Nutrient feedback between regions is shown in coloured arrows.